ELSEVIER

Ceramics International 27 (2001) 251–260

CERAMICS INTERNATIONAL

www.elsevier.com/locate/ceramint

Unlubricated friction and wear behavior of low-pressure plasma-sprayed ZrO_2 coating at elevated temperatures

J.H. Ouyang *, S. Sasaki

Mechanical Engineering Laboratory, AIST/MITI, 1-2 Namiki, Tsukuba, Ibaraki 305-8564, Japan

Received 6 March 2000; received in revised form 3 April 2000; accepted 5 May 2000

Abstract

The unlubricated friction and wear behavior of low pressure plasma-sprayed (LPPS) ZrO_2 coating were studied by using a standard SRV wear test system with reciprocating motion against sintered Al_2O_3 ceramic sphere from room temperature to 800°C. Microstructural observations showed that ZrO_2 splats appeared as fine lamellae structures together with small amounts of Al_2O_3 and SiO_2 inclusions with different gray levels in the back-scattered electron (BSE) mode. The friction and wear of ZrO_2 coating showed a strong dependence on temperature, changing from a low to a high wear regime with the increase of temperature. ZrO_2 coating exhibited low friction and wear at room temperature and 200°C. However, when temperature was increased to above 400°C, friction and wear of the coating increased rapidly and reached a maximum at 600°C together with significant noise and distinct vibration caused by severe surface fracture. Intersplat fracture and surface fatigue of ZrO_2 splats were demonstrated to be the dominated wear mechanism at room temperature. Delamination caused by subsurface crack propagation and inclusion cracking was the dominated wear mechanism at 600°C. Above 700°C, recrystallization and abrasive wear in the form of removal of fine ZrO_2 grains became the dominated wear mechanism together with local plastic flow and viscous deformation.

Keywords: ZrO_2 coating; Plasma spraying; Friction and wear at elevated temperatures

1. Introduction

The potential benefits of zirconia ceramics such as high hardness and wear resistance, excellent resistance to oxidation, hot corrosion and mechanical erosion, and high thermal insulation properties, have attracted considerable attentions in the industrial applications of heat engine and gas turbine parts, and aerospace seal and lubrication systems [1–4]. Zirconia ceramics are generally considered to be damage-tolerant and therefore should be expected to give more consistent tribological performance [2]. Despite wide scientific interest, the friction and wear of ZrO_2 ceramics at extreme conditions are still poorly understood. Previous studies [1] on bulk magnesium–partially stabilized zirconia (Mg–PSZ) ceramics showed that during unlubricated sliding wear at temperatures up to 700°C the wear resistance varied with temperature and sliding speed by as much as to three orders of magnitude and was associated with phase transformation on the frictional interface. The coefficient of friction increased distinctly with the increase of temperature up to 500°C [3]. The unlubricated coefficients of friction greater than 0.4 for ZrO_2-based ceramics have been found in the temperature range from 25 to 1000°C [4]. Both strength and toughness of toughened zirconia ceramics decrease with increasing temperature, which restricted the load-bearing applications of these materials to low and intermediate temperatures. However, strengh and toughness is not the only factor which affects the tribological behavior of ZrO_2 ceramics. Some authors [5] suggested that high wear rates in zirconia may be associated with surface fracture on a very fine scale. A 2 mol.% yttria–tetragonal zirconia polycrystals (2Y–TZP) has a greater wear rate than a 3Y–TZP drawing die. An intergranular fracture mechanism in the 2Y sample but a plastic deformation mechanism in the 3Y sample dominated the wear. Since the higher toughness ceramic (2Y) had undergone surface fracture whilst the lower toughness ceramic (3Y) had not, the transformation of the tetragonal phase to the monoclinic phase and the associated volume increase had

* Corresponding author. Tel.: +81-298-617196; fax: +81-298-617007.
E-mail address: ouyangjh@hotmail.com (J.H. Ouyang).

0272-8842/01/$20.00
PII: S0272-8842(00)00072-9

resulted in eruption of the surface fracture and therefore an increase in the wear rate.

Typically, plasma spraying is the main method used for depositing a wide range of thermal barrier coatings and wear resistant coatings. Wear behavior of as-sprayed zirconia coatings have been widely studied under a wide range of test conditions, which showed considerably different experimental results. Previous studies [6–8] indicated that wear mechanisms of plasma-sprayed ZrO_2 coatings could be fatigue spalling, plastic deformation, material transfer and brittle fracture, depending on the nature of the material and the test conditions applied. Wear test by using a ball-on-inclined plane scratch method [9] demonstrated that in the case of a plasma-sprayed ZrO_2 coating, beyond the critical load, cracks initiate at the surface and propagate into the subsurface at an angle about 30° to the sliding surface.

In a test of plasma-sprayed 8 wt.% Y_2O_3–ZrO_2 coatings, conducted in a reciprocating sliding wear tester at a temperature of 800°C, the wear behavior was significantly affected by the monoclinic to tetragonal phase transformation [10]. It was also reported that an increase in the amount of phase transformation from t' to t occurred on the worn surface and wear debris with an increase in temperature to 800°C, and this was related to the lower wear loss with increasing temperature.

It appears that the tribological properties of ZrO_2 coatings are very sensitive to the microstructure, especially the porosity, microcracking and inclusions in as-sprayed coatings [6,7,9,10]. Clearly, there remain many unanswered questions about the role of temperature in the wear behavior of zirconia ceramic coating. High temperature tribological applications of ZrO_2 coatings often exclude the use of conventional lubricants. Therefore, better understanding of unlubricated sliding wear of ZrO_2 coating at elevated temperatures is definitely required. This paper presented an investigation into the effects of temperature on friction and wear of ZrO_2 coating and in particular reported the detailed wear behavior at elevated temperatures.

2. Experimental procedure

2.1. Specimen preparation and microstructural observations

The substrate material was stainless steel AISI 304 which was machined into $\phi 25 \times 7$ mm circular plates. The chemical composition of substrate was (wt.%): 0.06 C, 0.5 Si, 1.0 Mn, 18.5 Cr, 9.0 Ni and balance Fe. The coating material studied was 8 wt.% Y_2O_3 stabilized ZrO_2 with a particle size of 10–45 μm. The coatings have been deposited on steel AISI 304 by low-pressure plasma spray (LPPS). Before spraying, the substrate material was sand-blasted with aluminum oxide grits and then cleaned in an ultrasonic bath with benzine and acetone. All substrates were plasma-sprayed by using Ar/He plasma gases. The chamber was first brought below 10 Pa, and argon gas was then added to the desired pressure. In order to find the optimum parameters for the processing technique to produce adherent coating, different parameters such as arc current, gas content and flow rate, heating temperature and powder feeding rate were carefully adjusted in different ways by the computer controlling systems. The plasma spraying parameters were optimized as arc voltage 45 V, arc current 750 A, argon gas pressure 0.343 MPa, helium gas pressure 1.03 MPa, spraying distance 150 mm and powder feed rate 15–20 g/min.

Microstructural characterization of the as-sprayed layers was observed by using optical microscope and JEOL-JSM6400F scanning electron microscope equipped with energy dispersive X-ray analysis system (EDX) and operated at 10 kV. The chemical composition of as-sprayed coatings was analyzed with a CAMECA SX-100 electron probe microanalyzer (EPMA). For SEM observations, plasma sprayed specimens were carefully sectioned using an abrasive wheel flooded with water. The cross-sectioned samples were ground and then polished successively by using a standard metallographic procedure. Before grinding, an epoxy adhesive was applied to ensure that the coatings did not peel off during grinding and polishing.

2.2. Wear test

The wear test was conducted using a standard SRV wear test system with reciprocating motion against 10 mm sintered Al_2O_3 ceramic sphere. The coating specimen was located in the testing chamber in a fixed specimen holder. The load affecting the specimen was generated by a motor spring system and recorded by a measuring unit. The oscillating, horizontal movement was generated by a moving coil drive. The force transducer thus enabled measurements of the frictional forces at the sliding surface and recorded the course of the coefficient of friction during the complete test run. Test temperatures from room temperature to 900°C can be easily controlled by thermocouple. The wear conditions were given as 30–80 N load, 10 Hz frequency, test temperature from room temperature to 800°C, 1 mm stroke and 1 h test duration. All the test runs were conducted without lubrication in laboratory air. The wear tracks of the coatings were also investigated by a surface texture measuring instrument to measure the depth and width of the tracks. The morphology of worn surfaces and the cross-longitudinal sections of worn specimens were observed by optical microscopy and SEM.

2.3. Vickers hardness analysis of the as-sprayed coating

Specimens were indented by using an AKASHI MVK-E Vickers hardness tester with a 9.8 N test load

and a Vickers diamond pyramid indenter on the polished cross-sections or surfaces. Optical microscopy was used to measure the dimension of indentation diagonal and the observed crack length, which extended from the corners of the indentation. The hardness of as-sprayed ZrO_2 coating was measured to be 650–727 HV on the polished cross-sections. On the polished surface of ceramic layer, no distinct change in hardness of the ceramic layer (699–724 HV) was found. The small variations in hardness value of the ZrO_2 coatings were attributed to the porosity and the microcracks in as-sprayed coatings. The crack patterns resulting from Vickers indentation in as-sprayed ZrO_2 coatings by indenting a polished cross-section were mainly identified as crack type I (Fig. 1a), where the dominant cracks were parallel to the substrate and emanate from or near one or two of the impression diagonal corners. This pattern can be viewed as resulting from the indent position in a dense portion of the coating where complete transmission of indentation stresses to the surrounding material would be expected to produce a Boussinesq stress field [11], with the resultant surface traces near one or both of the impression diagonals. In the present study, indents on the polished surfaces (Fig. 1b), which were made perpendicular rather than parallel to the substrate, did not produced any cracks emanating from four corners of the indent under 9.8 N indented load. When a high indented load was employed, it was possible to cause the typical crack pattern on the polished surface. Crack length had several attractions as a tool for characterizing the fracture toughness and mechanical response of brittle ceramic coating. Of course, crack length mainly depended on the indented load. When 9.8 N load was used in this investigation, crack length on polished cross-section was 0.08–0.1 mm. The fracture toughness of as-sprayed ZrO_2 coatings can be calculated to be 3.2–4.5 MPa $m^{1/2}$, if using an estimated elastic modulus of 284 GPa for yttria-stabilized zirconia according to the following equation [12,13]:

$$K_{IC} = 0.016(E/H)^{1/2}(P/C^{3/2}). \quad (1)$$

Where K_{IC} is the fracture toughness, MPa $m^{1/2}$; P is the indenter load, N; E is the Young's modulus, GPa; H is the hardness, GPa; and C is the crack length, mm.

The hardness was also measured on the polished cross-section of as-sprayed ZrO_2 coatings after 1 h wear test at 700°C. Slight decrease in hardness values (613–648 HV) was found as comparison to the original coating. Only very fine and short cracks emanating from the corner of the impression diagonal were observed. This indicated that partial thermal stress in as-sprayed coating was effectively relieved by high temperature wear process. Similar results of hardness were also observed within the coating after 800°C wear test.

3. Results

3.1. Microstructural features of as-sprayed coating

The typical features of as-sprayed ZrO_2 coating with a thickness of about 210 μm were shown in Fig. 2. The coating exhibited a porous and lamellar structure. Optical microscopy observations on polished cross-sections (Figs. 1a and 2a) showed a perfect connection at the coating/substrate interface. The main defect structures in the coating were pores, some microcracks (Fig. 2b and c), internal boundaries and foreign inclusions. Microcracking in ZrO_2 lamellae may be caused by the great volume changes associated with the low temperature ZrO_2 phase transformation from tetragonal to monoclinic during cooling. EDX spot analyses indicated that the dark inclusions (Fig. 2b) with different gray levels from ZrO_2 lamellae were rich in aluminum oxide, which may come from the original powder. A few fine silica lamellae were also detected within the coating by EDX. High magnification BSE photograph (Fig. 2b)

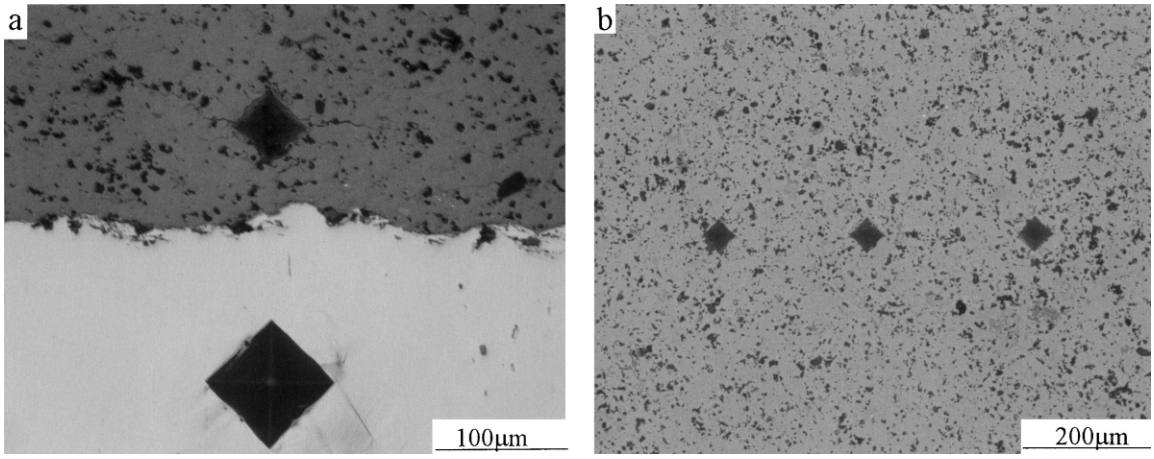

Fig. 1. Vickers indents showing the crack pattern within ZrO_2 coating: (a) on the polished cross-section; (b) on the polished surface.

showed more complicated microstructures with different gray levels at the interfacial regions. Different compositional images on the polished cross-section were shown in Fig. 3. Several Al_2O_3 lamellae and silica inclusions were detected within the coating. Some oxides of aluminum and silicon existed at the interfacial regions. EDX spot analyses at the interface also demonstrated the presence of a very few discontinuous oxidized products of iron and chromium from the substrate. However, high temperature wear test up to 700°C did not destroy the strongly adhesive bonding from the micrographs shown in Section 3.5.

3.2. Friction behavior of ZrO_2 coating against 10 mm sintered Al_2O_3 ceramic sphere

Friction coefficients of ZrO_2 coating at room temperature and different loads were shown in Fig. 4. It can be seen that friction coefficients of ZrO_2 coating was about $\mu = 0.25$–0.4 at room temperature. With the increase of load from 30 to 80 N, coating exhibited a decrease trend in friction coefficient. In all tests at room temperature, the wear process was very quiet and was associated with a relatively low friction coefficient. With the increase of test time, friction coefficients of the coating exhibited a slight decrease trend at all test loads.

Fig. 5 showed the relationship between the friction coefficients of coatings and test time at different temperatures. At 200°C, the friction coefficient of coating was slightly lower than that at room temperature ($\mu = 0.25$–0.34). But at 400°C or higher temperatures, a gradual increase in noise, vibration and friction coefficient was distinctly found. This increase was associated with the severe surface fracture. Friction coefficient exhibited great variations during the wear duration. Steady state was characterized by a rapidly changing friction coefficient, substantial surface noise and vibration at the elevated temperatures. When test temperature was increased to 400°C, average friction coefficient increased to 0.634. At 600°C, friction coefficients of ZrO_2 coating

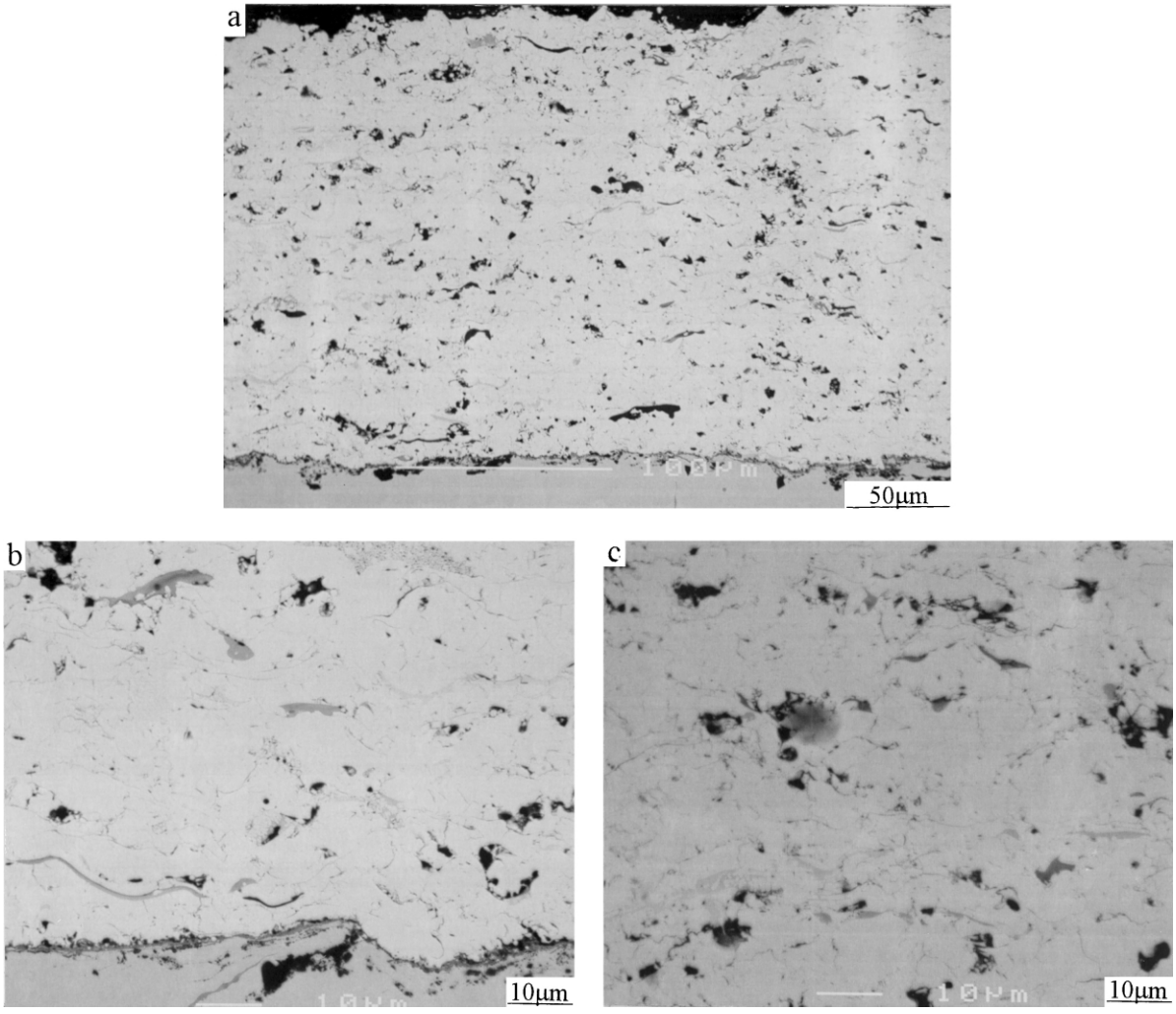

Fig. 2. Typical features of as-sprayed ZrO_2 coating: (a) cross section; (b) morphology of the inclusions and the coating/substrate interface; (c) high magnification micrograph showing the pores and microcracks.

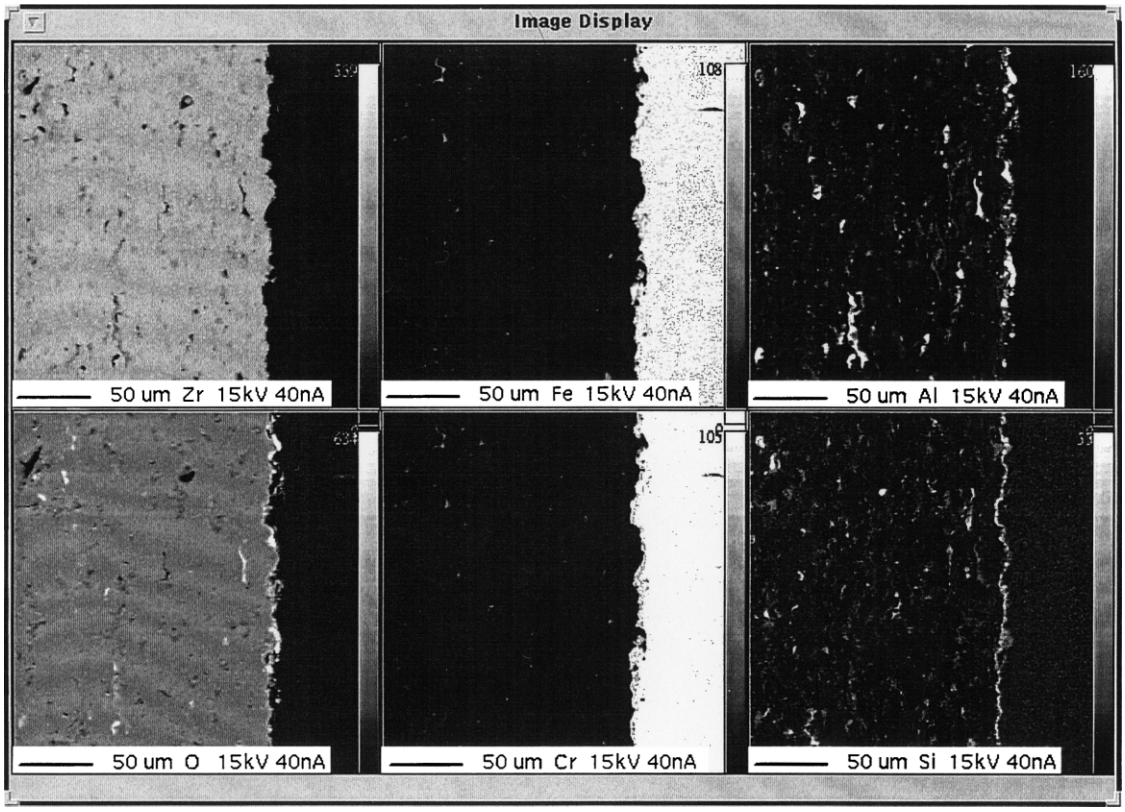

Fig. 3. Different compositional images on the polished cross-section of ZrO_2 coating.

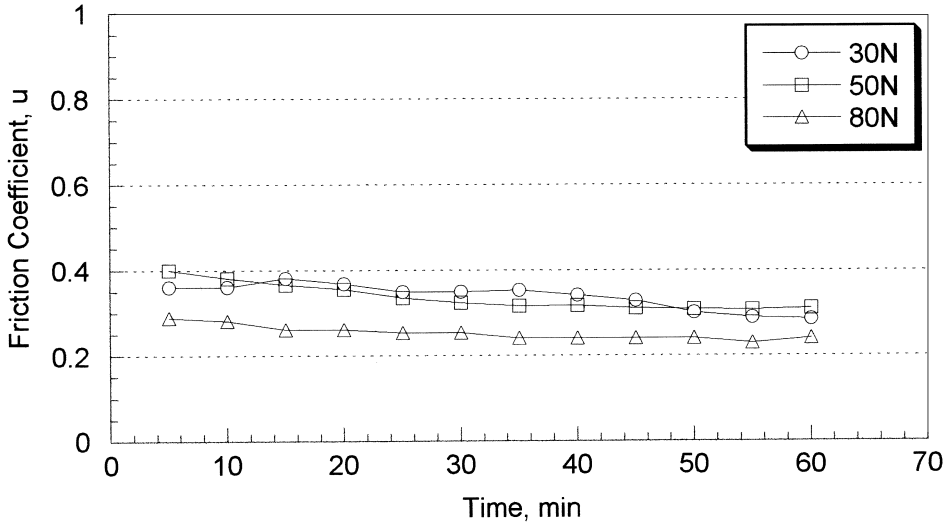

Fig. 4. Friction coefficients of ZrO_2 coating at room temperature and different loads.

reached a maximum value of 0.997. But when temperature continued to increase to 700 and 800°C, friction coefficients were 0.831 and 0.967, respectively.

3.3. Wear depth of as-sprayed ZrO_2 coating

Wear depth of ZrO_2 coating at room temperature and different loads was shown in Fig. 6. It can be seen that wear depth of the coating was about 38–62.5 μm at room temperature. With the increase of load from 30 to 80 N, the coating exhibited an increase trend in wear depth because of the increasing real tribocontact area although the low friction coefficients were observed at higher loads.

Fig. 7 showed the effect of test temperature on the wear depth of ZrO_2 coatings. Wear depth had a mini-

mum value of 53 μm at 200°C. At 400°C, wear depth of the coating were measured to be 145 μm. At 600°C, wear depth reached a maximum value of 151 μm. When temperature was up to 800°C, wear depth was 141 μm. Similar results were also obtained for the wear width of coating.

3.4. Observations of worn surfaces of as-sprayed ZrO_2 coating

Worn surfaces of selected ZrO_2 coatings were observed by optical microscope and SEM. The worn surfaces of the coatings at 50 N load and different test temperatures were shown in Fig. 8. At room temperature, typical brittle fracture was observed on the worn surface without evidence of plastic deformation under this experimental condition (Fig. 8a). Large wear sheets together with fine and irregular wear particles on the tribocontact surfaces were considered to result from surface fatigue, brittle fracture and crumbling. One of the important features on the worn surface for room temperature test was intersplat fracture or splat pull-out. The original plasma-sprayed morphology at many local surface regions can be clearly observed as shown by the arrows in Fig. 8a. Fig. 8b and c illustrated the morphology of worn surface after 600°C wear test. Brittle microcracking, delamination, local plastic deformation and occasional splat pull-out were observed on the worn surface. It was worth noting that a lot of primary cracks as shown in Fig. 8b and c were full of smooth and viscous inclusions. EDX spot analyses at these regions detected the presence of silicon and aluminum besides zirconium and oxygen elements. Delamination was observed from the upper left side in Fig. 8b to be caused

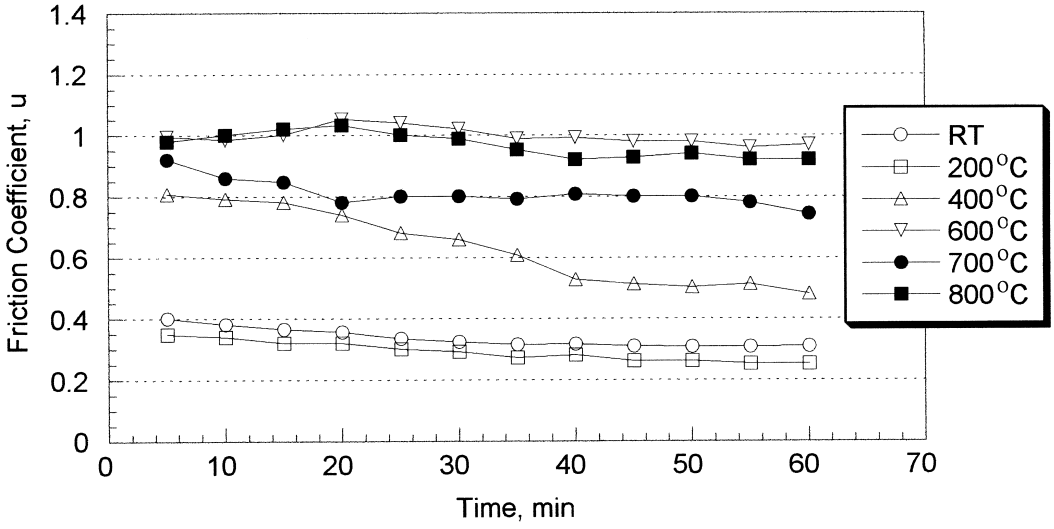

Fig. 5. Relationship between the friction coefficient of ZrO_2 coating and test time at different temperatures and 50 N load.

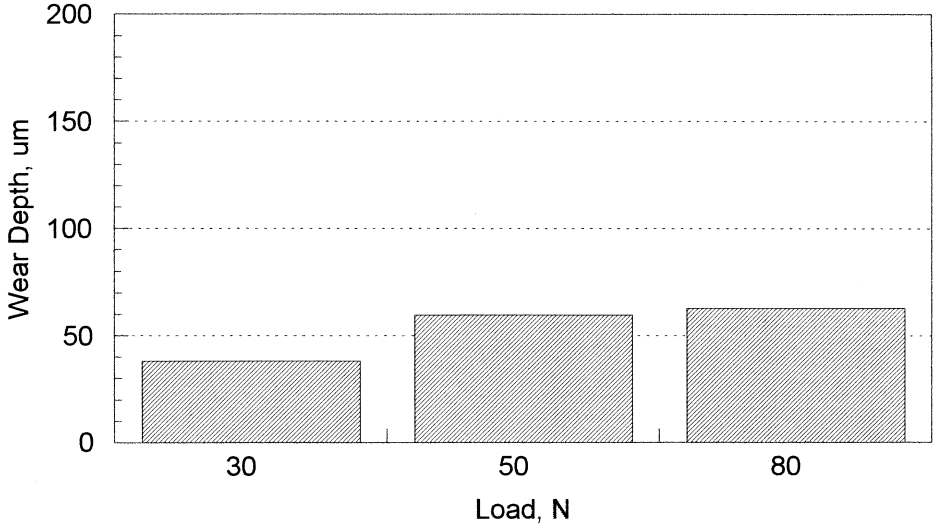

Fig. 6. Wear depth of ZrO_2 coating at room temperature and different loads.

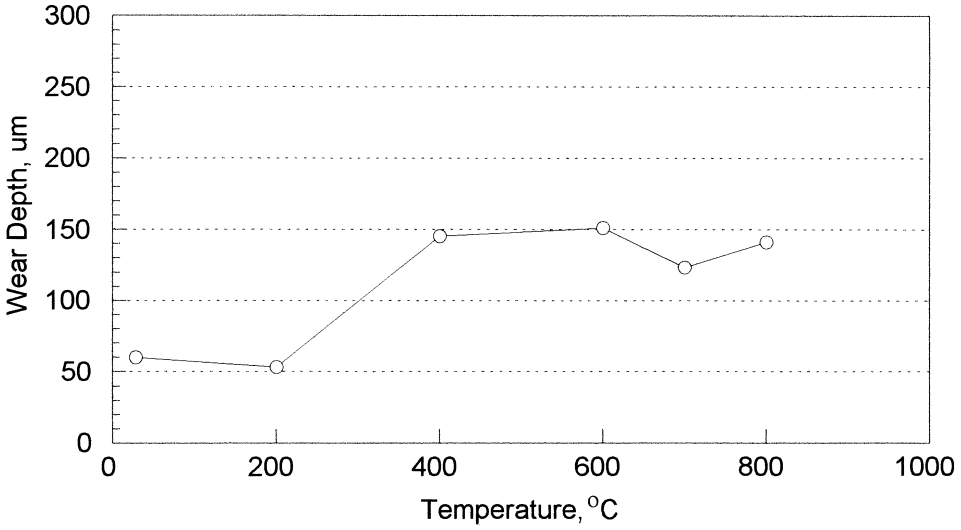

Fig. 7. Effect of test temperature on the wear depth of ZrO_2 coating at 50 N load.

by this kind of cracks containing the inclusions. The fine particles were formed by extensive plastic deformation and fracture of the microcracked lamellae as shown in Fig. 8c. When test temperature was increased to 700°C, worn surface (Fig. 8d) was entirely covered with fine particles together with the evidence of local plastic smearing and viscous deformation (Fig. 8e). Severe viscous flow and crumbling of recrystallized grains within the ZrO_2 splats because of high frictional heat under initial high contact stress. From Fig. 8e and f, the size of recrystallized grain clusters was very fine. Individual ZrO_2 recrystallized grain was much less than 1 μm. Clear evidence has been presented in this study which shows that no plastic deformation type wear mechanism had occurred in this region. Moreover, evidence of microfracture type mechanisms was found, and would have been clearly visible in these experiments.

3.5. Morphology of cross-longitudinal sections of worn specimens

Fig. 9 showed the cross-longitudinal sections of the wear tracks on selected ZrO_2 coatings at 50 N load and different temperatures. From Fig. 9a, the micrograph showed that the presence of wear debris adhered to the surface in localized region with a size of several micrometers was about to detach from the surface as shown by the arrow. Fine cracks with an angle to the surface were also observed within the subsurface layer after room temperature test. At 400°C, a large fracture pit caused by the detached wear particles can be clearly found in the surface regions shown in Fig. 9b. At 600°C, extended transverse crack, which was parallel to the worn surface, was found within the subsurface layer (Fig. 9c). This crack was an indication of the depth of crack initiation and propagation before particle detachment. The delamination crack in this case was generated by joining microcracks and micropores in the as-sprayed coating. After repeated passes which cause repeated surface relaxation, cracks propagated by breaking the bridges between grains, either towards the surface or in the band of the subsurface layer with an excessive defects. In addition, two distinct fracture pits were considered to result from severe delamination of coating. From Fig. 9d, no obvious surface damage could be observed on the longitudinal cross-sections after 700°C wear test. Fine microstructural feature was observed within the subsurface layers. It suggested that high temperature wear process caused the nucleation and recrystallization of ZrO_2 grains. No evidence of plastic deformation has been presented from the longitudinal cross-sections.

4. Discussion

The wear process of ZrO_2 coating at room temperature and 200°C produced lower friction coefficient and material removal rates comparing to those at elevated temperatures described previously. The worn surface at room temperature appeared to be similar to a fracture surface including intersplat fracture, crumbling of coating and splat pull-out. Larger chip-like debris resulted from surface or subsurface fatigue fracture, while smaller chip-like debris was caused by intersplat fracture.

The friction and wear results at 600°C showed that the dominated wear mechanism of ZrO_2 coating was delamination although a few plastic deformation was also observed on the worn surface. This delamination-controlled wear mechanism led to a distinct increase in both friction coefficient and wear rate. The microcracks, which developed in the subsurface, connected and pro-

pagated to generate large cracks after repeated passes. These microcracks were possible to result from the tetragonal to monoclinic phase transformation within the subsurface. Another possible site for microcrack nucleation was the brittle glass-phase or inclusion, which was located at the intersplats. These inclusions, which formed as a consequence of the contaminated surfaces of the starting powders, served in many cases as a path for microcrack propagation as shown in Fig. 8c.

The differences in friction and wear resistance at 700°C under dry-sliding conditions depended on coating properties such as fracture toughness, hardness and also on the interfacial temperature between the splats. Because of the low thermal conductivity of zirconia coating, a rapid tem-

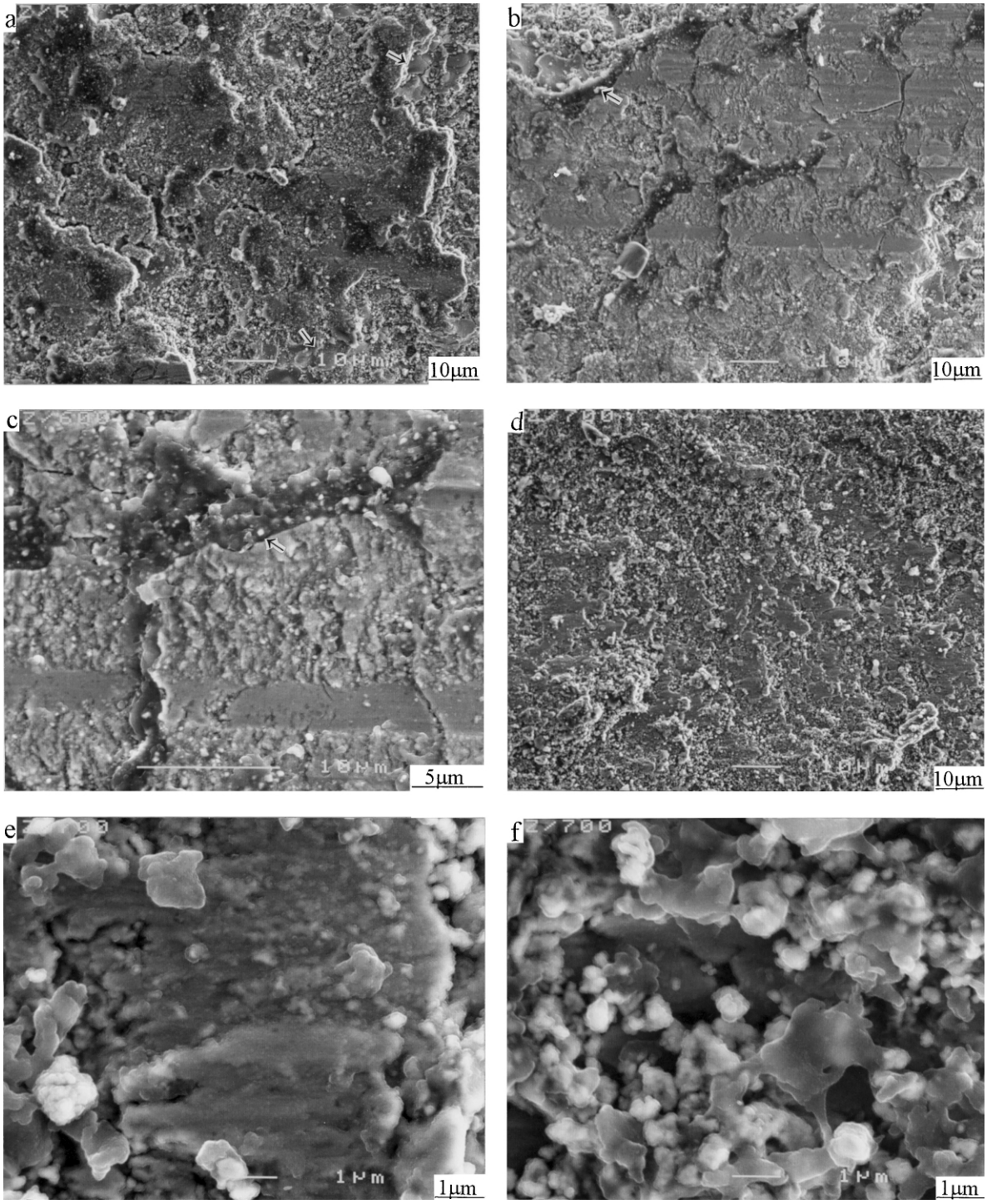

Fig. 8. Worn surfaces of selected ZrO_2 coatings at 50 N load and different test temperatures: (a) room temperature; (b) 600°C; (c) high magnification of b; (d) 700°C; (e,f) high magnifications of d.

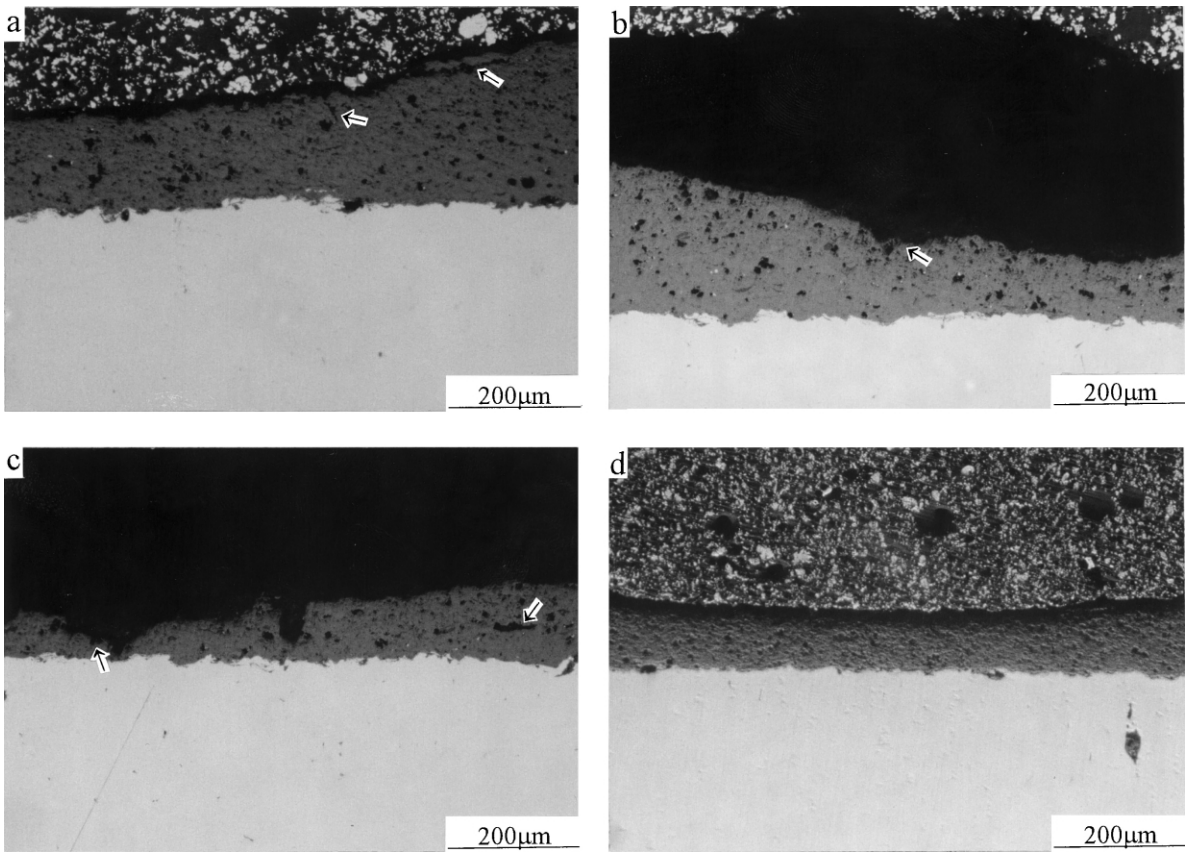

Fig. 9. Longitudinal cross-sections of the wear tracks of selected ZrO_2 coatings at 50 N load and different temperatures: (a) room temperature; (b) 400°C; (c) 600°C; (d) 700°C.

perature increase at asperities may be caused by frictional heating. On the worn surface or within the subsurface layer, recrystallization process of ZrO_2 can easily take place due to the poor thermal conductivity of ZrO_2 at 700°C from Fig. 8e and f. Due to these thermal processes and high real contact stress, microfracture at the grain boundaries can be easily observed, especially in the area of internal volume defects such as flaws, voids and weak grain boundaries. Therefore, the recrystallizing and abrasive wear process of the surface and subsurface layers can be expected to be the dominated wear mechanism at 700°C. During this wear process, the friction was also highly accompanied by significant noise and distinct vibration caused by the severe surface fracture. Local viscous flow and deformation of coating were also responsible for the material removal of ZrO_2 grains.

5. Conclusions

1. Within the plasma-sprayed coating, ZrO_2 splats were observed as fine lamellae structures together with small amounts of Al_2O_3 and SiO_2 inclusions with different gray levels in the back-scattered electron (BSE) mode. Some microcracks, pores and internal boundaries were observed in ZrO_2 coating. The hardness and fracture toughness of as-sprayed ZrO_2 coating were found to be 650–727 HV and 3.2–4.5 MPa $m^{1/2}$, respectively.
2. ZrO_2 coating exhibited low friction and wear at room temperature and 200°C. However, when test temperature was increased to above 400°C, friction and wear of the coating increased distinctly and reached a maximum at 600°C together with substantial noise and distinct vibration caused by severe surface fracture.
3. Intersplat fracture and surface fatigue of ZrO_2 splats were demonstrated to be the dominated wear mechanism at room temperature. Delamination caused by subsurface crack propagation and inclusion cracking was the dominated wear mechanism at 600°C. However, recrystallization and abrasive wear in the form of removal of fine ZrO_2 grains became the dominated wear mechanism together with local plastic flow and viscous deformation above 700°C.

Acknowledgements

The authors would like to thank Dr. Umeda, Dr. Alam and Mrs. Saito for their kindly help in specimen preparation, SEM observations and wear test. One of the authors, Dr. J.H. Ouyang, also expresses his thanks to Agencies of Industrial Science and Technology (AIST) of Japan for the award of AIST research fellowship.

References

[1] V. Aronov, Friction induced strengthening mechanisms of magnesia partially stabilized zirconia, Journal of Tribology 109 (1987) 531–536.
[2] W.M. Rainforth, R. Stevens, A transmission electron microscopy study of wear of magnesia partially stabilized zirconia, Wear 162 (164) (1993) 322–331.
[3] R.H. Hannink, M.J. Murray, H.G. Scott, Friction and wear of partially stabilized zirconia: basic science and practical applications, Wear 100 (1984) 355–366.
[4] M. Woydt, K.H. Habig, High temperature tribology of ceramics, Tribology International 22 (1989) 75–87.
[5] I. Birkby, P. Harrison, R. Stevens, The effect of surface transformation on the wear behavior of zirconia TZP ceramics, Journal of the European Ceramic Society 5 (1989) 37–46.
[6] Y.L. Wang, Y.S. Jin, S.Z. Wen, The analysis of the friction and wear mechanisms of plasma-sprayed ceramic coatings at 450°C, Wear 128 (1988) 265–276.
[7] H. Ahn, J. Kim, D. Lim, Tribological behaviour of plasma-sprayed zirconia coatings, Wear 203 (204) (1997) 77–87.
[8] H.S. Ahn, O.K. Kwon, Wear behavior of plasma-sprayed partially stabilized zirconia on a steel substrate, Wear 162 (164) (1993) 636–644.
[9] Y.L. Wang, S.M. Hsu, P. Jones, Evaluation of thermally-sprayed ceramic coatings using a novel ball-on-inclined plane scratch method, Wear 218 (1998) 96–102.
[10] J.Y. Kim, D.S. Lim, H.S. Ahn, High-temperature wear of plasma-sprayed ZrO_2–Y_2O_3 coatings, Journal of the Korean Ceramic Society 30 (1993) 1059–1065.
[11] B.R. Lawn, M.V. Swain, Microfracture beneath point indentation in brittle solids, Journal of Materials Science 10 (1975) 113–122.
[12] G.R. Anstis, P. Chantikul, B.R. Lawn, D.B. Marshall, A critical evaluation of indentation techniques for measuring fracture toughness: I. Direct crack measurements, Journal of American Ceramic Society 64 (9) (1981) 533–538.
[13] G.K. Beshish, C.W. Florey, F.J. Worzala, W.J. Lenling, Fracture toughness of thermal spray ceramic coatings determined by the indentation technique, Journal of Thermal Spray Technology 2 (1) (1993) 35–38.